Step-Index Optical Fiber Made of Biocompatible Hydrogels

*Myunghwan Choi, Matjaž Humar, Seonghoon Kim, and Seok-Hyun Yun**

The limited penetration of light into biological tissue poses a formidable challenge in many applications of light in biomedicine. Although a few approaches, such as near-infrared spectral window[1] and wave-front shaping,[2] have been shown to improve light penetration, optical waveguides, particularly optical fibers, represent the current gold-standard solution in clinical uses.[3] However, most light-guiding systems are based on conventional solid-state optical materials, such as glasses and inorganic plastics, which unfortunately are not compatible with the biological system.[4] To overcome this limitation, there have been continuing efforts to develop optical waveguides using biocompatible materials, such as poly(ethelyene glycol) (PEG),[5] silk,[6] agarose gel,[7] and even bacteria.[8] However, the light-guiding structures demonstrated to date have not yet been considered for biomedical applications because of the following limitations. First, their light-guiding efficiency is not sufficient to deliver light over an organ-scale distance, which is over 10 cm for humans. The $1/e$ attenuation lengths of the waveguides ranged from only tens of micrometers[8] to a few centimeters.[5] Equally importantly, the previous approaches used a single material with uniform refractive index. In such core-only waveguides, guiding is achieved by total internal reflection at the interface between the material and the surrounding medium. As a result, the guiding efficiency is considerably degraded when the waveguides are introduced into living biological tissues, where the local refractive index in the tissue (1.33–1.51) in contact with the core is comparable to or higher than that of the core material.[9]

In this communication, we demonstrate a new type of optical fibers that solve these technical limitations. First, we employ a core-clad structure with an overall step index profile, which enable us to confine light within a core surrounded by a clad layer. We demonstrate excellent guiding efficiency and stability within living biological tissues. Second, we use biocompatible hydrogels for the core and clad, for the first time to our knowledge. Besides their desirable mechanical flexibility, the hydrogels allow us to incorporate various functional fluorophores and nanoparticles into their porous structure to build various types of specialty fibers for biomedical applications including in vivo optical sensing and light-induced therapy.

For low-loss light guiding, the core and clad must have high optical transparency, and the core should have higher refractive index than the cladding. To meet these basic requirements, we investigated two widely used biocompatible hydrogels: PEG and alginate.[10] We have previously reported that the optical properties of PEG hydrogels were highly dependent on precursor concentration.[5] At concentrations of PEG-diacrylate (PEGDA) (700 Da) higher than 15%, the optical transparency of PEG hydrogels after UV-induced polymerization increased with the monomer concentration (**Figure 1**a). The measured refractive index (n) of the hydrogels was in good agreement with calculated values by a linear weighted sum of the refractive indices of constituent materials (PEGDA, n = 1.46; water, n = 1.331), increasing linearly with the precursor concentration (Figure 1b). The PEG hydrogels showed slightly higher refractive indices than the precursor solutions due to shrinkage during photopolymerization. At low precursor concentrations of alginate (1–4% w/v), the optical transparency of alginate hydrogels decreased with the concentration (Figure 1c). The refractive index of alginate hydrogels increases as a linear function of precursor concentration and was close to that of water (n = 1.331) due to their high water content (Figure 1d). Considering both the refractive index and transparency, we decided to use 80–90% w/v PEG hydrogels for the core and 1–2% w/v alginate hydrogels for the cladding.

We developed a two-step process to fabricate the core and cladding (**Figure 2**a). First, the core was fabricated by using a platinum-cured silicone tube as a mold. The inner diameter of the tube mold determined the diameter of the core (Figure 2b). Precursor solution for PEG hydrogel was injected into the tube and photo-crosslinked by exposure to ultraviolet light. After the mold was swollen in dichloromethane for 30 min, the core was extracted. Then, the core was dipped in a sodium alginate and calcium chloride solution, typically two to four times until multilayered alginate cladding is formed to a desired thickness (typically 100–150 μm). The thickness of the each clad layer was controlled by the temperature of the dipping solution. Thinner clads are formed at higher temperature due to lower viscosity of the solution. It typically took about 2 h to complete the entire process. This fabrication process was reproducible and scalable (Figure 2c).

Prof. M. Choi, Dr. M. Humar, Dr. S. Kim, Prof. S.-H. Yun
Harvard Medical School and Wellman Center for Photomedicine
Massachusetts General Hospital
65 Landsdowne St, UP-5, Cambridge, MA 02139, USA
E-mail: syun@hms.harvard.edu
Prof. M. Choi
Global Biomedical Engineering
Sungkyunkwan University
Center for Neuroscience and Imaging Research
Institute for Basic Science
2066 Seobu-ro, Jangan-Gu, Suwon-Si, Gyeong Gi-Do, South Korea
Dr. M. Humar
Condensed Matter Department
J. Stefan Institute
Jamova 39, SI-1000 Ljubljana, Slovenia
Dr. S. Kim
Graduate School of Nanoscience and Technology
Korea Advanced Institute of Science and Technology
291 Daehak-Ro, Yusong-Gu, Daejon 305-701, South Korea

DOI: 10.1002/adma.201501603

© 2015 WILEY-VCH Verlag GmbH & Co. KGaA, Weinheim

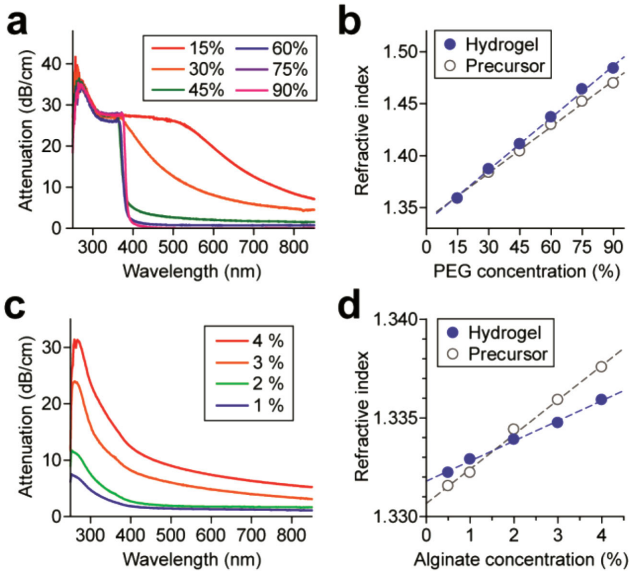

Figure 1. Optical properties of bulk hydrogels in cuvettes. a) Measured attenuation coefficients and b) refractive indices of PEG hydrogels made with a monomer size of 700 Da at concentrations of 15–90% w/v. c) Absorption spectra and d) refractive indices of alginate hydrogels at concentrations of 1% –4% w/v.

We evaluated the light-guiding properties of the fabricated hydrogel fibers. Laser light at a wavelength of 492 nm was coupled to a hydrogel fiber, and the side-scattering pattern of the light transmitting along the fiber was imaged when the fiber was placed in air (Figure 2d) or embedded between thin porcine tissue slices (Figure 2e). From the axial intensity profile of side-scattered light, the propagation loss of the hydrogel fiber at 492 nm was measured to be 0.32 ± 0.02 dB cm^{-1} in air and 0.42 ± 0.01 dB cm^{-1} in tissue (Figure 2f). The slightly lower loss in air is presumably due to the contribution by light leaked from the core (due to defects) but guided farther through the clad-air interface. By contrast, a single-index core-only PEG hydrogel fiber fabricated without alginate coating showed a significantly higher loss of 1.15 dB cm^{-1} in tissue. In terms of $1/e$ penetration depth, the step-index hydrogel fibers offer light guidance over 10 cm in the visible spectrum (Figure 2g).

The high permeability of hydrogels allowed us to incorporate functional molecules into the fibers (**Figure 3**a). The pore size of a PEG hydrogel made with 700 Da monomers is approximately 1.5 nm, which permit small molecules to penetrate into the hydrogels by diffusion.[11] Dye molecules, such as rhodamine 6G, were easily loaded into the core by dipping the distal end of the core in dye solution prior to cladding encapsulation (Figure 3b). The incorporated dye absorbs coupled excitation light, adding additional attenuation to the fiber. The absorptive attenuation is linearly proportional to concentration and extinction coefficient. In case of 1×10^{-6} M rhodamine 6G, the fiber attenuation at the absorption peak (530 nm) is estimated to be ≈0.1 dB cm^{-1} but it becomes negligible in the spectral region other than the absorption band (e.g., 0.002 dB cm^{-1} at 600 nm). This diffusion-based solution doping process does not involve any chemical reactions and is therefore reversible. For example, photobleached dyes could be removed from the fibers by washing, and active dyes could be replenished.

Alternatively, more robust functionalization by covalent bonding is also possible by incorporating complementary reactive functional groups. We encapsulated avidin into the core, and the fabricated fiber was doped by dipping it in a solution containing biotin-conjugated fluorophores. As an example, we doped a fiber with three different biotin-conjugated fluorophores, Atto 488, Atto 520, and Atto 565, respectively, in three distinct positions along the fiber (Figure 3c). This was achieved by applying 1 µL dye droplets to the fiber. When blue laser light (491 nm) was coupled into the fiber, it emitted bright fluorescence at distinct spectra from the dye-doped regions (Figure 3c).

Molecules larger than the pore size can be physically entrapped by mixing them in the precursor solution before crosslinking. Using this method, we embedded gold nanoparticles (GNPs) with a diameter of 50 nm and, therefore, a plasmonic resonance-enhanced absorption peak at a wavelength of 532 nm. When the GNP-doped fiber was pumped with continuous-wave 532 nm laser light, significant heat was generated from GNP's and the temperature of the fiber increased by ≈16 °C in 1 min with a coupled optical power of 0.6 W (Figure 3d). At the same pumping condition, a control fiber without GNPs showed a much less temperature increase of ≈3 °C (Figure 3e). This result demonstrates the potential of the hydrogel fiber for photothermal applications.

We next explored the possibility of using a dye-doped hydrogel fiber for optical amplification. We loaded rhodamine 6G in the core of a fiber using the diffusion method described above. For optical pumping, a Q-switched laser light was illuminated to a 5-mm segment of the fiber by focusing through a cylindrical lens (**Figure 4**a). The output emission from the fiber tip was collected through an objective lens and analyzed by a spectrometer with a cooled charge coupled detector (CCD). At pump fluences less than 5 µJ mm^{-2}, the typical fluorescence emission of rhodamine 6G with a spectral width of ≈50 nm was measured (Figure 4b,c). As the pump intensity increased, the emission power increased superlinearly, accompanying narrowing of spectral width down to 6 nm in full-width-half-maximum (FWHM) (Figure 4b,c). This phenomenon, known as amplified spontaneous emission (ASE), results from the amplification of guided fluorescence light along the fiber.[12]

Another mode of light amplification was observed in the tangential direction of the fiber through whispering gallery mode (WGM) guiding.[13] To generate WGM lasing, we arranged the optical geometry so that the direction of pumping and collection are the same in the transverse plane of the fiber (Figure 4d). At pump intensities above threshold, sharp emission spectral peaks appeared at wavelengths of ≈585 nm (Figure 4e). The output energy increased superlinearly with a distinct threshold at ≈80 µJ mm^{-2} (Figure 4f). Camera images showed predominant light extraction at the core-clad interface above laser threshold, as expected from bidirectional (clockwise and counter clockwise) WGM oscillations (Figure 4f, inset). Below threshold, fluorescence was emitted uniformly from the entire core. Lasing was suppressed when we intentionally disrupted the WGM path by cutting the fiber to a D-shape. These results collectively suggest WGM lasing.

© 2015 WILEY-VCH Verlag GmbH & Co. KGaA, Weinheim

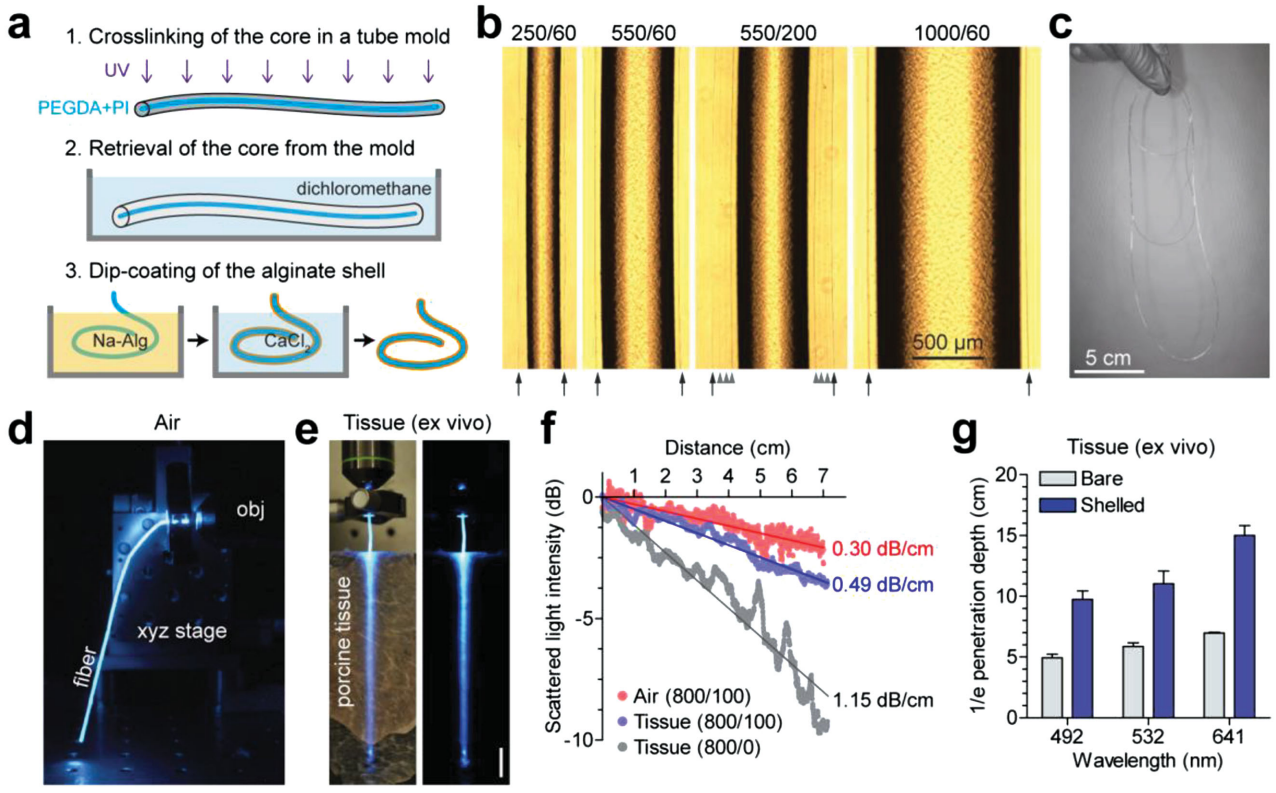

Figure 2. Fabrication of core-cladded fibers. a) Fabrication steps. Step 1: PEG hydrogel is formed by photo-crosslinking in a tube mold. Step 2: the core is extracted from the tube by swelling the tube in dichloromethane. Step 3: the alginate hydrogel clad layer is added by dip coating. Step 3 can be repeated to obtain a desired clad thickness. b) Phase-contrast images of four hydrogel fibers with different sizes, immersed in distilled water. Arrows indicate the outer clad-water interface and arrowheads indicate interfaces between alginate layers formed by multiple dip coating. The numbers on top represent the thickness of the core and the clad in μm (i.e., 250/60 indicates 250 μm core diameter and 60 μm clad thickness; the outer diameter is thus 370 μm). The third image (550/200) shows a four-layer cladding. c) A photograph of a 1 m long fiber. d) Light guidance in air. Blue laser light (492 nm) was coupled to a hydrogel fiber (800/100) through a 10× objective lens (obj). e) Light guidance of a fiber (800/100) sandwiched between two thin porcine tissue slices. Scale bar: 1 cm. f) Propagation loss of three different fibers. g) Corresponding 1/*e* propagation distances of the bare (800/0) and shelled (800/100) fibers.

Potential medical applications of the hydrogel fibers include deep-tissue light-based therapies based on photothermal or photodynamic therapy.[14] The high flexibility of hydrogel fibers allows them to be implanted and integrated in tissues easily or

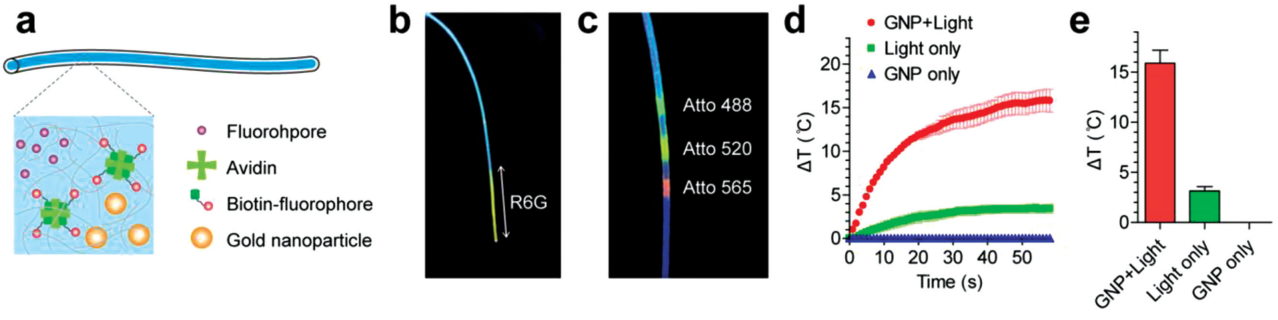

Figure 3. Functionalized hydrogel fibers. a) A schematic for functionalization of the core. Small-molecular fluorophores can be loaded through passive diffusion. Immobilization of the fluorophores can be achieved by introducing reactive groups (e.g., avidin) in the core. Larger objects, such as gold nanoparticles (GNP) can be physically trapped during the fabrication of the hydrogel core. b) A fluorescence image of a dye-doped fiber. Rhodamine-6G was loaded in the fiber by dipping the tip in a solution of the fluorophore. When blue laser was coupled, the dye-doped region emits yellow fluorescence from excited rhodamine-6G molecules. c) A fluorescence image of a fiber doped with three different fluorophores, Atto 488, 520, and 565, respectively, along the fiber. The biotin-conjugated fluorophores were incorporated into the avidin-encapsulated core. d,e) Photothermal operation of a GNP-doped fiber. Green laser (532 nm and 800 mW) was coupled to the fiber to induce photothermal heating. Temperature was measured using a thermocouple in contact with the fiber.

© 2015 WILEY-VCH Verlag GmbH & Co. KGaA, Weinheim

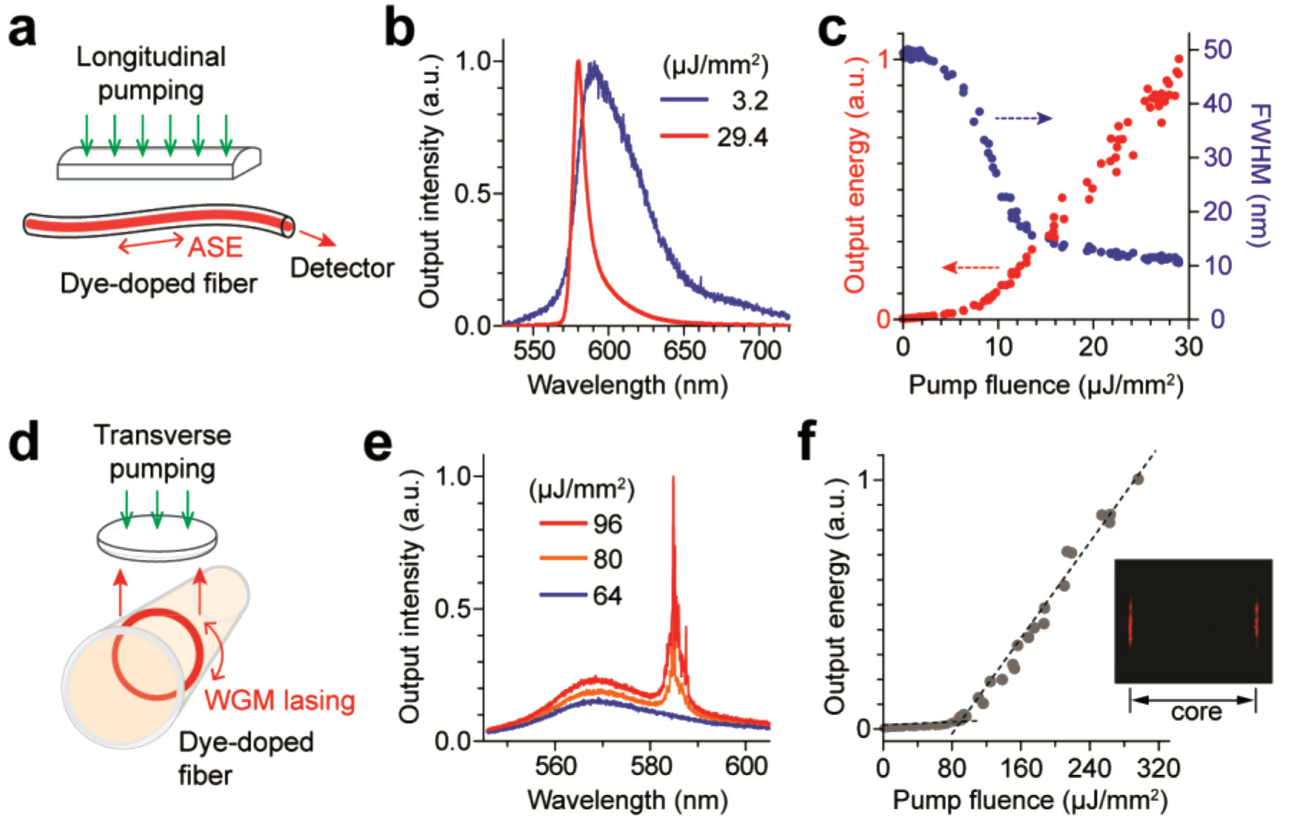

Figure 4. Light amplification in a dye-doped fiber. The core was doped with rhodamine-6G and pumped with a Q-switched laser at 535 nm. a) A setup for amplified spontaneous emission (ASE). Approximately 5 mm length of the fiber was pumped, and the guided ASE output at the end of the fiber was analyzed. b) Output spectra measured at two different pump levels. c) Output energy (red) and spectral width (blue) as a function of pump fluence. d) A setup for whispering-gallery-mode (WGM) lasing. The red ring illustrates the optical paths of the laser modes oscillating along the circumferential interface between the core and the cladding. e) Output spectra measured at three different pump levels. f) The output power curve showed a distinct lasing threshold about 80 μJ mm^{-2}. Inset: a side-view image of the fiber above laser threshold. The red region indicates the laser light that was leaked from the fiber by scattering and recorded in a camera.

inserted through natural opening, such as the gastrointestinal tracts. We tested this feasibility in live mice. A hydrogel fiber was inserted into the intestine through the rectum (**Figure 5**A), which was not possible with a conventional silica optical fiber because of its stiffness. Laparotomy confirmed efficient delivery of light to the distal end despite the relatively small bending radius of the fiber.

We also tested the feasibility of optical sensing of blood oxygenation levels by absorbance spectroscopy. Two hydrogel fibers were implanted in subcutaneous tissues of an anesthetized mouse with their tips separated by 5 mm from each other. One of the fibers delivered excitation light at 560 and 640 nm into the tissue, and the other fiber collected the light diffused through the tissue (Figure 5b). As the oxygen level of the supplied gas was modulated by switching between nitrogen and oxygen, the changes in the optical intensity signal at 560 and 640 nm were measured and, using Beer Lambert law, converted to relative oxy- and deoxyhemoglobin concentrations. As expected, inhalation of nitrogen caused sudden drop in oxygen tension in the blood, i.e., a decrease in oxyhemoglobin and an increase in deoxyhemoglobin. The oxygen tension was reversed by inhalation of oxygen (Figure 5c).

Although our current fibers successfully achieved organ-scale transmission (>10 cm), the performance can be further improved. The primary cause of loss is thought to be the surface roughness (≈1 μm) of the tube mold. Improved mold surface would lower the waveguide loss significantly. Besides the step-index structure, other types, such as a double clad guiding structure or even a gradient index profile, should be achievable by using more than two materials or a solution doping technique. Furthermore, it may be possible to fabricate fibers with much smaller core diameters for single-mode operation. Much thinner sizes at even sub-micrometer scale may be feasible by microfluidics or electrospinning techniques.[15] Injectable hydrogel, such as thermoresponsive sol–gel hydrogels, may allow minimally invasive implantation through a needle by forming a hydrogel fiber structure in situ.[16] Formation of complex microstructured fibers in situ may also be feasible by introducing advanced microfluidic techniques on the needle. Furthermore, hydrogels with highly stretchable or self-healing properties could be adapted to improve mechanical stability.[17]

In summary, we have described the fabrication, optical characteristics, and applications of core-clad step-index hydrogel optical fibers. Low-loss light guiding (<0.42 dB cm^{-1}) over the

© 2015 WILEY-VCH Verlag GmbH & Co. KGaA, Weinheim

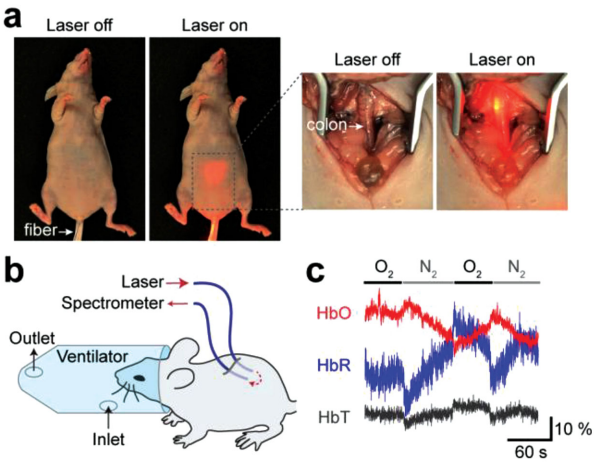

Figure 5. Demonstration of uses in vivo. a) Pictures of a mouse with a hydrogel fiber administered to the colon through the rectum. The emission of red laser (640 nm) at the distal end of the fiber is seen through the skin and confirmed by abdominal laparotomy. b,c) Reflectance oximetry of tissues. b) Two hydrogel fibers—one for excitation and the other for collection—were implanted subcutaneously in an anesthetized mouse to measure the intrinsic optical absorption signal in response to oxygen/nitrogen ventilation. c) Typical time-lapse traces of the calculated concentrations of oxy-hemoglobin (HbO), deoxy-hemoglobin (HbR), and total hemoglobin (HbT = HbO + HbR).

entire visible spectrum was achieved in vivo. The hydrogel core allowed various functional materials, such as organic molecules and plasmonic nanoparticles, to be incorporated for the generation of fluorescence, amplified spontaneous emission and WGM lasing, as well as photothermal heat generation. We expect that the biocompatible, functional hydrogels fibers will have broad impact in the field of photomedicine by bringing photonic tools toward in vivo system.

Experimental Section

Fabrication of Core-Clad Fiber: Platinum-cured silicone tubes (Cole Parmer) with inner diameters of 250–1000 μm were used as a mold for the core. Precursor solution composed of 80% w/v PEGDA (700 Da; Sigma–Aldrich), 5% w/v 2-hydroxy-2-methyl-propiophenone (Sigma–Aldrich) in distilled water was injected in the tube through a syringe adapted with a syringe filter with 0.45 μm pore. The PEG hydrogel was formed by photo-crosslinking the solution with exposure to UV (365 nm, 5 mW cm^{-2}; Spectroline) for 5 min. The tube with the crosslinked core was immersed in dichloromethane for 30 min, and then the core was isolated from the swollen tube. The core was immersed in distilled water at least for 1 h to remove unreacted chemicals. To form the clad layer, the core was immersed in alginate solution (2% w/v; Sigma–Aldrich) and then in calcium chloride solution (100×10^{-3} M; Sigma–Aldrich). This procedure was repeated to form a multilayer clad. Successful fabrication of the core-clad fiber was checked by phase-contrast microscopy (Olympus).

Optical Characterization: Refractive indices of hydrogels were measured with a digital refractometer (Sper Scientific). Hydrogels were prepared in a standard 1 cm-wide poly(methyl methacrylate) disposable cuvettes, and optical attenuation was measured using a scanning spectrophotometer over a spectral range from 250 to 1000 nm (Thermo Scientific). To make homogeneous alginate gels in a cuvette, sodium alginate (1–4% w/v; Sigma–Aldrich) was slowly gelated with a combination of $CaCO_3$ (15×10^{-3} M; Sigma–Aldrich) and δ-gluconolactone (15×10^{-3} M; Sigma–Aldrich) as described previously.[18]

Optical Setup for Optical Amplification Measurement: For dye doping, the fiber core with diameter of 800 μm was immersed in rhodamine-6G solution (0.1% w/v) for over 12 h, and then the alginate clad was added by dip coating. The fiber was mounted on a slide glass and placed on a three-axis micrometer. Laser pulses from optical parametric oscillator (Quanta Ray MOPO-700, Spectra Physics; 535 nm, 5 ns, 10 Hz) were illuminated to the fiber from the side for optical pumping, and the output emission from the fiber was collected through an objective lens and analyzed with a spectrometer (Andor, 300 mm focal length).

Animal Experiments: 8 to 12 weeks-old BALB/c nude mice (Jackson Laboratory) were used after being anesthetized by intraperitoneal injection of ketamine (100 mg kg^{-1}) and xylazine (10 mg kg^{-1}). For the experiment demonstrating implanted light source, the descending colon of the mouse was flushed several times with warm saline and the fiber was introduced through the rectum.[19] Abdominal laparotomy was followed to gain visual access to the descending colon where fiber tip was placed. For reflectance oximetry, two fibers were subcutaneously implanted, and oxygen and nitrogen was alternately ventilated with an interval of 30–60 s. The change in reflectance at 560 and 640 nm in wavelength was measured respectively. The relative change in intensity, $\Delta I/I$, was converted to oxy and deoxyhemoglobin levels as previous described.[20] In brief, attenuation for each wavelength was represented as linear summation of absorptions by oxy and deoxyhemoglobin using Beer–Lambert law, and concentration for each hemoglobin type was decomposed by solving the set of linear equations. All animal experiments were performed in compliance with institutional guidelines and approved by the subcommittee on research animal care at the Harvard Medical School.

Acknowledgements

The authors thank Prof. Xiangwei Zhao for discussions. This work was funded by the U.S. National Institutes of Health (Grant Nos. P41EB015903 and R21EB013761) and Marie Curie International Outgoing Fellowship N° 627274 within the 7th European Community Framework Programme.

Received: April 3, 2015
Revised: May 3, 2015
Published online: June 5, 2015

[1] a) G. Hong, S. Diao, J. Chang, A. L. Antaris, C. Chen, B. Zhang, S. Zhao, D. N. Atochin, P. L. Huang, K. I. Andreasson, *Nat. Photonics* **2014**, *8*, 723; b) M. Choi, K. Choi, S.-W. Ryu, J. Lee, C. Choi, *J. Biomed. Opt.* **2011**, *16*, 046008.
[2] N. Ji, T. R. Sato, E. Betzig, *Proc. Natl. Acad. Sci. USA* **2012**, *109*, 22.
[3] a) G. Keiser, F. Xiong, Y. Cui, P. P. Shum, *J. Biomed. Opt.* **2014**, *19*, 080902; b) M. J. Gora, J. S. Sauk, R. W. Carruth, K. A. Gallagher, M. J. Suter, N. S. Nishioka, L. E. Kava, M. Rosenberg, B. E. Bouma, G. J. Tearney, *Nat. Med.* **2013**, *19*, 238.
[4] S. Nizamoglu, M. C. Gather, S. H. Yun, *Adv. Mater.* **2013**, *25*, 5943.
[5] M. Choi, J. W. Choi, S. Kim, S. Nizamoglu, S. K. Hahn, S. H. Yun, *Nat. Photonics* **2013**, *7*, 987.
[6] S. T. Parker, P. Domachuk, J. Amsden, J. Bressner, J. A. Lewis, D. L. Kaplan, F. G. Omenetto, *Adv. Mater.* **2009**, *21*, 2411.
[7] A. Jain, A. H. Yang, D. Erickson, *Opt. Lett.* **2012**, *37*, 1472.
[8] H. Xin, Y. Li, X. Liu, B. Li, *Nano Lett.* **2013**, *13*, 3408.
[9] S. L. Jacques, *Phys. Med. Biol.* **2013**, *58*, R37.
[10] A. S. Hoffman, *Adv. Drug Delivery Rev.* **2002**, *54*, 3.

© 2015 WILEY-VCH Verlag GmbH & Co. KGaA, Weinheim

[11] G. M. Cruise, D. S. Scharp, J. A. Hubbell, *Biomaterials* **1998**, *19*, 1287.
[12] P. Yang, G. Wirnsberger, H. C. Huang, S. R. Cordero, M. D. McGehee, B. Scott, T. Deng, G. M. Whitesides, B. F. Chmelka, S. K. Buratto, *Science* **2000**, *287*, 465.
[13] a) M. Humar, M. Ravnik, S. Pajk, I. Muševič, *Nat. Photonics* **2009**, *3*, 595; b) S. McCall, A. Levi, R. Slusher, S. Pearton, R. Logan, *Appl. Phys. Lett.* **1992**, *60*, 289.
[14] A. F. Bagley, S. Hill, G. S. Rogers, S. N. Bhatia, *ACS Nano* **2013**, *7*, 8089.
[15] A. L. Yarin, E. Zussman, J. Wendorff, A. Greiner, *J. Mater. Chem.* **2007**, *17*, 2585.
[16] a) C. H. Choi, H. Yi, S. Hwang, D. A. Weitz, C. S. Lee, *Lab Chip* **2011**, *11*, 1477; b) B. Jeong, S. W. Kim, Y. H. Bae, *Adv. Drug Delivery Rev.* **2002**, *54*, 37.
[17] a) J.-Y. Sun, X. Zhao, W. R. Illeperuma, O. Chaudhuri, K. H. Oh, D. J. Mooney, J. J. Vlassak, Z. Suo, *Nature* **2012**, *489*, 133; b) A. Phadke, C. Zhang, B. Arman, C.-C. Hsu, R. A. Mashelkar, A. K. Lele, M. J. Tauber, G. Arya, S. Varghese, *Proc. Natl. Acad. Sci. USA* **2012**, *109*, 4383.
[18] C. K. Kuo, P. X. Ma, *Biomaterials* **2001**, *22*, 511.
[19] M. Choi, S. H. Yun, *Opt. Express* **2013**, *21*, 30842.
[20] M. Suh, S. Bahar, A. D. Mehta, T. H. Schwartz, *NeuroImage* **2006**, *31*, 66.

© 2015 WILEY-VCH Verlag GmbH & Co. KGaA, Weinheim